Elevated CO_2 increases sensitivity to ultraviolet radiation in lacustrine phytoplankton assemblages

Cristina Sobrino,[a,1,]* P. J. Neale,[a] J. D. Phillips-Kress,[a] R. E. Moeller,[b] and J. A. Porter[c,2]

[a] Smithsonian Environmental Research Center, Edgewater, Maryland
[b] Miami University, Oxford, Ohio
[c] Lehigh University, Bethlehem, Pennsylvania

Abstract

   This study tests the effects of elevated CO_2 and ultraviolet radiation (UVR) on phytoplankton photosynthesis through in situ incubations in Lake Giles, Pennsylvania. In a first experiment, CO_2 was supplied from a tank to simulate atmospheric CO_2 concentrations predicted in scenarios of future global change. In a second experiment, elevated CO_2 conditions were obtained by the mineralization of added colored dissolved organic matter (CDOM) of terrestrial origin (400 μmol L^{-1} final concentration). The results demonstrated that for natural assemblages from Lake Giles, atmospheric CO_2 concentrations similar to those predicted for the end of the century can increase primary productivity up to 23% in the absence of photoinhibition. However, elevated CO_2 concentrations also increased sensitivity of phytoplankton to UVR, making cells more susceptible and increasing photoinhibition. Increased sensitivity was observed in samples incubated with the artificial CO_2 supply as well as with the CDOM addition, the latter resulting in CO_2 partial pressures close to three times present atmospheric levels. Photosynthetic rate modeled for elevated CO_2 and midday solar exposure just below the lake surface was 17% of potential production compared with 21% under usual CO_2 levels in the lake, resulting in similar rates between phytoplankton assemblages grown under high and low CO_2 levels. Understanding the effect on primary productivity of the interaction between factors that may be affected by global change is essential to predict future changes in ecosystems and climate.

   The increase in atmospheric CO_2 caused by anthropogenic production since 1970 has been propagated to the aquatic systems through the surface layer (Sabine et al. 2004), reaching values 1.4 times higher than the preindustrial concentrations. On the other hand, global change affects solar ultraviolet B (UVB, 280–320 nm) and ultraviolet A (UVA, 320–400 nm) penetration in surface waters through changes in the stratospheric ozone concentration, cloud cover, and changes in the colored part of dissolved organic matter (CDOM) (for review *see* Zepp et al. 2007). The latter becomes especially relevant in freshwater ecosystems and coastal waters. CDOM concentration and composition controls the penetration of UV radiation (UVR) into water bodies, but CDOM is also photodegraded by solar UVR (Zepp et al. 1995; Moran and Zepp 1997; Moran et al. 2000), resulting in loss of color (photobleaching) and the enhancement of UVR exposure to aquatic organisms. In addition, UVR-induced photomineralization of CDOM releases CO_2 and increases the biological availability of DOM, which can be used as an energy source for microbial respiration (Moran et al. 2000; De Lange et al. 2003; Lennon 2004). All these findings indicate that UVR penetration in aquatic environments can reinforce global climate change directly, by increasing atmospheric CO_2, reducing phytoplankton carbon fixation, and increasing CDOM photomineralization, and indirectly,

through the production of biolabile compounds for microbial respiration.

   The interaction between elevated CO_2 concentrations and incident UVR (280–400 nm) affects phytoplankton metabolism, producing different responses from those expected from the addition of the individual effects (Sobrino et al. 2005, 2008). Nevertheless, the in situ response of natural assemblages is still unknown. In general, it is expected that long-term elevation of CO_2 in the absence of photoinhibition would increase phytoplankton growth and carbon fixation (Hein and Sand-Jensen 1997; Ibelings and Maberly 1998; Riebesell et al. 2000), but natural samples have not always shown a significant response (Tortell and Morel 2002). Conversely, UVR-caused decrease in areal primary productivity can be up to 30% and varies with the sensitivity of phytoplankton to UVR (Pienitz and Vincent 2000; Helbling et al. 2001; Neale et al. 2001). The sensitivity of phytoplankton photosynthesis to UVR, i.e., the change in photosynthesis per unit UV exposure, is related to the balance between the damage and repair capacity of the cells. It varies among species but it can also be affected by natural environmental factors such as temperature (Sobrino and Neale 2007), light acclimation history (Villafañe et al. 2004), and nutrient and CO_2 availability, among others (Litchman et al. 2002; Sobrino et al. 2008). Furthermore, the increase or decrease in sensitivity of photosynthesis to UVR produced by some external conditions is not always directly related to the increase or decrease in photosynthesis under nonphotoinhibitory exposures. For example, in *Nannochloropsis gaditana*, a picoplanktonic marine species, increased CO_2 did not increase carbon fixation under nonphotoinhibitory

---

* Corresponding author: sobrinoc@uvigo.es
  Present address:
  [1] University of Vigo, Vigo, Spain
  [2] University of the Sciences in Philadelphia, Philadelphia, Pennsylvania

photosynthetically active radiation (PAR, 400–700 nm) exposures but decreased sensitivity to UVR when compared with cells grown under atmospheric levels of CO_2 (i.e., cells became more resistant to UVR) (Sobrino et al. 2005). In contrast, elevated CO_2 concentrations increased carbon fixation in the estuarine diatom *Thalassiosira pseudonana*, but CO_2 elevation also increased sensitivity to UVR (i.e., cells became less resistant to UVR) (Sobrino et al. 2008). The opposite responses observed between these species regarding sensitivity to UVR was mainly attributed to differences in the degree of acclimation to elevated CO_2 conditions and it is explained in detail in Sobrino et al. (2008). In this sense freshwater ecosystems with consistent CO_2 supersaturation of the water column provide phytoplankton assemblages that are long-term acclimated to high CO_2 conditions and are an interesting tool to test future scenarios of elevated CO_2 concentrations (Cole et al. 1994; Granéli et al. 1996). Even so, the resulting primary production under high CO_2 and UVR photoinhibitory exposures will ultimately depend on the degree of the maximum photosynthetic rates attained under nonphotoinhibitory exposures, the degree of sensitivity to UVR, and the irradiance and spectral composition of the light reaching the organisms.

In this study we analyze the interacting effects of UVR and high CO_2 concentrations on natural phytoplankton assemblages through in situ incubations performed during summer 2005 and 2006 in Lake Giles, Pennsylvania. Unlike the previous experiments with cultures, where the extra carbon pool was always supplied from a CO_2 tank, in this case we studied the effect on phytoplankton photoinhibition of CO_2 concentrations that were both artificially enhanced as well as naturally enhanced by photomineralization of added CDOM. These experimental approaches were intended to simulate future scenarios of climate change with elevated atmospheric CO_2 concentrations or increases in allochthonous inputs of organic matter, respectively. The latter might occur as climate warming promotes the soil development associated with altitudinal increase in treeline and vegetation, and as changes in precipitation regimes increase episodic storm events (Hauer et al. 1997; Hinton et al. 1997). We calculated photosynthetic rates in the presence and absence of UVR and estimated the biological weighting functions (BWFs) for the photoinhibition of lake phytoplankton (reviewed by Cullen and Neale 1997; Neale 2000).

Methods

Location and characteristics of Lake Giles—Lake Giles is a small (0.48 km²) postglacial lake formed in carbonate-poor Devonian sandstones and shales of the Pocono Plateau of northeastern Pennsylvania (41.4°N, 75.1°W, elevation 428 m above sea level). The water is slightly acidic (pH ca. 6.0 in 2005–2006) with low dissolved inorganic carbon (DIC, 25–33 μmol L^{-1}), as well as low dissolved organic carbon (DOC, ca. 100 μmol L^{-1}). The summer mixed layer (ca. 6 m) of the 24-m-deep lake is relatively UVR transparent and low in algal biomass (ca. 1 μg L^{-1} chlorophyll *a* [Chl *a*]). The lake is considered oligotrophic,

and mixed-layer phytoplankton are typically colimited by nitrogen and phosphorus in summer (R. E. Moeller unpubl.).

Setup—In summer 2005, a water sample was collected from 3-m depth in the lake at dusk using a pump at low pressure. After transportation to the laboratory (less than 1 h), the water was screened through 48-μm mesh to remove macrozooplankton grazers, and kept overnight in 20-liter microcosms with or without aeration (ca. 0.6 L min^{-1}) with 101.3 Pa CO_2 in air (0.1% CO_2 = 1000 parts per million by volume CO_2) until the start of the in situ incubation the next morning. Microcosms were translucent flexible polyethylene UVR-transparent containers (Nalgene® I-Chem Certified™ Series 300 low-density polyethylene Cubitainers™). Transmittance (T) into the cubitainers decreases progressively from 95%T at 700 nm to 84%T at 320 nm and 78%T at 290 nm. The cubitainers were previously incubated with lake water for 7 d and washed with 10% HCl. The air–CO_2-mixture gas tank was provided by Airgas. High-CO_2 and low-CO_2 (i.e., at lake CO_2 concentrations) microcosms were moored at 3-m depth for 6 d, tightly closed, and completely filled with sample to minimize air space. At this depth the incubated phytoplankton received approximately 10% of the incident UVR. An additional cubitainer, filled with 0.2-μm filtered lake water and aerated overnight similarly to the high-CO_2 samples, was also incubated in situ to quantify CO_2 diffusive loss from the high-CO_2 cubitainers. The experiment was performed in duplicate, with the duplicates starting on consecutive days (20 July 2005 and 21 July 2005). For each treatment, subsamples were collected at the beginning (T_0), near the middle, and after 6 d.

In summer 2006, water samples were again collected at 3 m but incubated near the surface (10 cm average depth) with and without an addition of CDOM for 6 d. The CDOM source was water from Beaver Pond, a small (0.09 km²), 12-m maximum depth, dystrophic pond located approximately 2 km northeast of Lake Giles, in an adjoining watershed. Beaver Pond is highly colored, with DOC concentrations ranging from 400 to 1200 μmol L^{-1} (varying seasonally) and a DOC-specific absorbance at 320 nm (a_{320} [DOC]$^{-1}$) of 4.15 m² g C^{-1}. Beaver Pond water was filtered through a 5-μm prefilter (Ace Hardware) and concentrated using a reverse osmosis unit built in the Morris Laboratory at Lehigh University according to Sun et al. (1995). Approximately 5% CDOM was added to Lake Giles water for a final DOC concentration of 400 μmol L^{-1} and a_{320} [DOC]$^{-1}$ of 3.35 m² g C^{-1}. Because of its chromophoric properties and proximity to Lake Giles, Beaver Lake water concentrated by reverse osmosis serves as a realistic approximation of the allochthonous CDOM input to Lake Giles and as an appropriate CDOM source for the experiments.

Lake water was passed through a 48-μm mesh to remove macrozooplankton as it was collected. A portion of this water, with and without added CDOM, was incubated in 2-liter, UV-transparent Teflon™ fluorinated ethylene-propylene bottles to assess the changes in phytoplankton sensitivity to UVR. In addition, bottles were covered with

UVR-opaque or UVR-transparent film to obtain two different UVR treatments with similar PAR: −UVR bottles were covered with Courtgard™ clear UV-absorbing film (CPFilm) that removes most of the UVR (50% cutoff at 400 nm) but allows the transmission of PAR, and +UVR bottles covered with Aclar clear film (Aclar fluoropolymer, Honeywell) that allows the transmission of full-spectrum PAR+UVR (98% of UVB 295–319 nm, 99% UVA 320–399 nm). PAR exposure in the two treatments was the same since both Aclar and Courtgard reflect about 5% at all wavelengths when immersed. A second portion of the water was further filtered through a 1-μm pore size polycarbonate (Nucleopore) filter to remove algae. This water, with and without added CDOM, was incubated in 250-mL Teflon bottles also with either Courtgard or Aclar.

Atmospheric conditions were quite constant during both years, with water temperature of 25.7°C ± 0.1°C at 3 m in 2005 (mean ± SEM, $n = 4$) and 21.2°C ± 1.4°C at the surface in 2006 (mean ± SEM, $n = 3$), and mainly clear days, excepting a stormy weather episode at the end of 2006 incubations.

DIC and CO_2 concentrations—Samples were collected in precleaned glass bottles, overflowing the bottle with the sample. They were kept in the dark at room temperature until analysis the same day using the method of Stainton (1973), in which a 25-mL sample is acidified and equilibrated with a N_2 headspace, then analyzed by gas chromatography (Shimadzu GC 8A chromatograph with PoraPak Q column). Water samples were analyzed in triplicate using Na_2CO_3 solutions as standards. An Orion pH meter with Ross™ combination electrode was used to measure pH. Samples were analyzed at room temperature after mixing in 1% by volume of pHisa™ ionic strength adjustor (™Thermo Fisher Scientific). CO_2 concentrations in the samples were calculated from total DIC concentrations, pH, and temperature using the program csys.m from Zeebe and Wolf-Gladrow (2001), applying dissociation constants for freshwater.

Chl a concentrations—Samples for Chl a and photosynthesis measurements were collected using a 1-liter polycarbonate bottle. Water samples (50 mL) were filtered in triplicate onto 25-mm glass fiber filters (GFF Whatman) for Chl a analysis. Filters were kept frozen until extraction following Pechar (1987). After 24 h at −10°C, fluorescence was measured (Sequoia-Turner model 112 or Turner 10-AU fluorometer) and calibrated with Chl a determined spectrophotometrically.

Taxonomic composition—Samples for phytoplankton enumeration were preserved with acid Lugol's solution, settled in Utermöhl chambers, and counted at 480× magnification using an Olympus IX71 microscope.

Photosynthetic responses to PAR—Photosynthesis–irradiance (P-E) curves for PAR-only exposure were obtained in a "photosynthetron" incubator using a modification of the protocol described by Lewis and Smith (1983). The temperature-regulated incubator uses a halogen lamp to assess the photosynthetic response to PAR ($n = 10$–12 intensities) as the conversion of inorganic $H^{14}CO_3^-$ (NEN sodium bicarbonate solution, 8.4 μCi ^{14}C μmol^{-1} C, Perkin Elmer) into organic (acid-stable) compounds over a 1-h incubation. Photosynthetic parameters, P_s^B and E_s, were estimated using nonlinear regression fitting of the equation:

$$P^B = P_s^B\left(1 - \exp\left[-\frac{E_{PAR}}{E_s}\right]\right) \qquad (1)$$

where P^B is photosynthesis normalized to Chl a content (g C [g Chl]$^{-1}$ h^{-1}), P_s^B is the light-saturated rate of photosynthesis, E_s is the saturation irradiance for PAR (μmol photons m^{-2} s^{-1}), and E_{PAR} is the PAR irradiance. Samples were incubated in 7-mL glass scintillation vials previously washed in 10% HCl and extensively rinsed. Each vial containing 6 mL of sample was inoculated with $H^{14}CO_3^-$ (ca. 0.02 μCi mL^{-1}) and capped immediately to avoid CO_2 exchange with the atmosphere during the incubation. Since each vial was inoculated individually (cf. Lewis and Smith 1983), total ^{14}C activity was determined by averaging the activity measured in four 100-μL subsamples taken from selected vials near the end of the incubation. PAR scalar irradiance was measured in vials filled with filtered lake water using 4-π sensor (QSL-2101, Biospherical Instruments).

Photosynthetic response to UVR: BWF and BWF$_T$/P-E model—Simultaneously with the photosynthetron incubations and using similar inoculation procedure and incubation time, the photosynthetic response to UVR was assessed using a special polychromatic incubator, the "photoinhibitron" (Cullen et al. 1992). A detailed description of the photoinhibitron incubator is given in Sobrino et al. (2008). Spectral irradiance in each cuvette was measured with a custom-designed spectroradiometer as previously described (Neale and Fritz 2001). The cuvettes were filled with 7 mL of sample, inoculated with $H^{14}CO_3^-$ (ca. 0.02 μCi mL^{-1}), and capped during exposure.

The BWF/P-E models are based on a PAR-only P-E curve equation, adding a term that represents inhibition of photosynthesis by UVR and PAR (Eq. 2). The inhibition term relates the effect of UVR to "weighted" irradiance, E_{inh}^* (i.e., spectral irradiance corrected by the biological effect or weight [Eq. 3]), and includes the BWF. The BWFs appear as a set of weighting coefficients, $\varepsilon(\lambda)$, that measure the strength of UVR action at each wavelength, therefore providing an estimation of the sensitivity to UVR exposure in relation to wavelength (reviewed by Neale 2000). For a step-by-step protocol for calculation of the BWFs for this study *see* Cullen and Neale (1997) and Sobrino et al. (2008). The BWF$_T$/P-E model (also called T model) with a saturating exponential P-E term was selected to predict photosynthesis in the presence of PAR and UVR exposures because it showed the highest R^2 and least bias in residuals. It is shown as:

$$P^B = P_s^B\left(1 - \exp\left[-\frac{E_{PAR}}{E_s}\right]\right)\min\left(1, \frac{1}{E_{inh}^*}\right) \qquad (2)$$

$$E_{inh}^* = \sum_{\lambda=280}^{400} \varepsilon(\lambda) \times E(\lambda) \times \Delta\lambda + \varepsilon_{PAR} \times E_{PAR} \qquad (3)$$

where min denotes the minimum function, E_{inh}^* is a dimensionless index for the biologically effective or weighted irradiance, $\varepsilon(\lambda)$ is biological weight ([mW m^{-2}]$^{-1}$) at wavelength λ, $E(\lambda)$ is spectral irradiance (mW m^{-2} nm^{-1}) at λ, and $\Delta\lambda$ is the wavelength resolution, 1 nm. Inhibition by PAR is included using a single broad band weight, ε_{PAR} ([W m^{-2}]$^{-1}$), for PAR irradiance (Cullen et al. 1992; Cullen and Neale 1997). BWFs were estimated from the measured rates of photosynthesis using nonlinear regression and principal component analysis (PCA) for samples from summer 2005 ($n = 2$, $m = 80$ spectral treatments per incubation), and the Rundel method for samples from summer 2006 ($n = 1$–3, $m = 40$ spectral treatments per incubation) (Rundel 1983; Cullen and Neale 1997). The Rundel fits with the smaller data sets produce BWFs with simpler shapes. Tests of fits using both the PCA method on $m = 80$ data set and Rundel method on a $m = 40$ subset of the same data showed that both methods gave similar trends in the variation of sensitivity between treatments. The BWFs shown in the manuscript correspond to the average BWF for each treatment with the SEM for each wavelength calculated from individual error estimates by propagation of errors.

Weighted irradiance in the in situ incubations (Teflon bottles) was calculated as

$$E_{inh}^* = \sum_{\lambda=280}^{400} \varepsilon(\lambda) \times E(\lambda) \times \Delta(\lambda) \times e^{-K_d(\lambda)z}$$
$$+ \varepsilon_{PAR} \times E_{PAR} \times e^{-K_{PAR}z}, \qquad (4)$$

whereas average weighed irradiance in the lake was

$$E_{inh}^* = \sum_{\lambda=280}^{400} \left[\varepsilon(\lambda) \times E(\lambda) \times \Delta(\lambda) \times \left(1 - e^{-K_d(\lambda)z}\right) \middle/ K_d(\lambda)z \right]$$
$$+ \varepsilon_{PAR} \times E_{PAR} \left(1 - e^{-K_{PAR}z}\right) / K_{PAR}z \qquad (5)$$

with z (m) representing the depth to the center of submerged bottles in Eq. 4 and the average mixed layer depth of the lake in Eq. 5, and $K_d(\lambda)$, K_{PAR} (m^{-1}) the attenuation coefficients in the UV and PAR, respectively. K_d's for the lake water column were estimated using a profiling UV radiometer (Biospherical Instruments BIC or PUV-500) and an exponential relationship between measured K_d's (305, 320, 340, 380 nm) and wavelength. Average K_d values during the 2005 experiments varied from K_d (305 nm) = 1.61 to K_d (400 nm) = 0.30, and in 2006 from K_d (305 nm) = 2.43 to K_d (400 nm) = 0.36. For samples incubated with a CDOM addition K_d's were estimated by adjusting the exponential decay of light absorption to the measurements assessed in situ using actinometers centered inside the Teflon bottles. Actinometry involved nitrite (UVA) and nitrate (UVB) solutions prepared and assayed as described by Jankowski et al. (1999). The solutions were exposed for a 6-h period

centered on solar noon in 1-cm-diameter borosilicate glass vials mounted in the center of the bottles.

Light measurements—Incident solar UVB radiation at the surface was measured by a Smithsonian SR18 UVB spectroradiometer, which has 18 channels in the wavelength range of 290 to 324 nm. Then, UVA and PAR spectral irradiances were calculated using a radiative transfer model (Ruggaber et al. 1994) implemented by the STAR software package (H. Schwander University of Munich) and adjusted for measured UVB as described by Fritz et al. (2008). UVB and UVA unweighted irradiances for a clear-day spectra at midday (21 July 2005) were 2.6 W m^{-2} and 50.9 W m^{-2}, respectively. UVR weighted irradiance calculated using the BWF for the inhibition of photosynthesis in the diatoms *Phaeodactylum tricornutum* (Cullen et al. 1992) and *T. pseudonana* (Sobrino et al. 2008), and the action spectra for deoxyribonucleic acid damage of Setlow normalized to 300 nm (Setlow 1974) were 1.44 (dimensionless), 3.04 (dimensionless), and 0.11 W m^{-2}, respectively.

Results

In experiments performed in summer 2005, where the CO_2 enrichment was supplied from a tank and algae received small UV exposure during the incubation, DIC in low CO_2 microcosms declined from average 28.3 μmol L^{-1} to 22.4 μmol L^{-1} after 6 d of incubation, and from average 64.1 μmol L^{-1} to 43.5 μmol L^{-1} in the high-CO_2 microcosms. Analysis of the carbon forms contributing to total DIC showed that at pHs of 5.98 ± 0.04 and 5.71 ± 0.04, for low CO_2 and high CO_2 (mean ± SEM, $n = 6$), respectively, CO_2 was predominant, with average partial pressures declining from 58.9 Pa to 46.8 Pa in the low-CO_2 microcosms, and from 160.9 Pa to 104.3 Pa in the high-CO_2 microcosms (Fig. 1A). Diffusive loss of CO_2 from the high-CO_2 cubitainer was 2.9 Pa d^{-1} (data not shown). Although the rate of CO_2 decrease (after correction for CO_2 leakage) was higher in the high-CO_2 than in the low-CO_2 microcosms, the increase in phytoplankton biomass, measured as bulk Chl a accumulation, was larger in the low-CO_2 than in the high-CO_2 microcosms, reaching average values of 3.4 μg L^{-1} and 2.8 μg L^{-1}, respectively (Fig. 1B) (repeated-measures ANOVA [RMANOVA], $p = 0.046$, $n = 2$, $m = 3$). At the start of the experiment, the cyanobacterium *Merismopedia tenuissima* made up 18% of the counted biovolume, and the chlorophytes *Sphaerocystis schroeteri* and *Elakatothrix gelatinosa* comprised respectively 74% and 8% of the total biovolume. Numerous much rarer taxa were not considered. Elevated CO_2 increased *Merismopedia* abundance 77% compared with low CO_2 conditions, whereas no significant differences were observed in *Sphaerocystis* or *Elakatothrix* with regard to CO_2 concentrations.

P-E curves in the absence of UVR showed that Chl a-specific carbon fixation increased significantly from the start to the end of the experiment (RMANOVA, $p = 0.0376$, $n = 2$, $m = 10$), and was higher in the high-CO_2 microcosms (Fig. 2) (RMANOVA, $p = 0.0002$, $n = 2$, $m =$
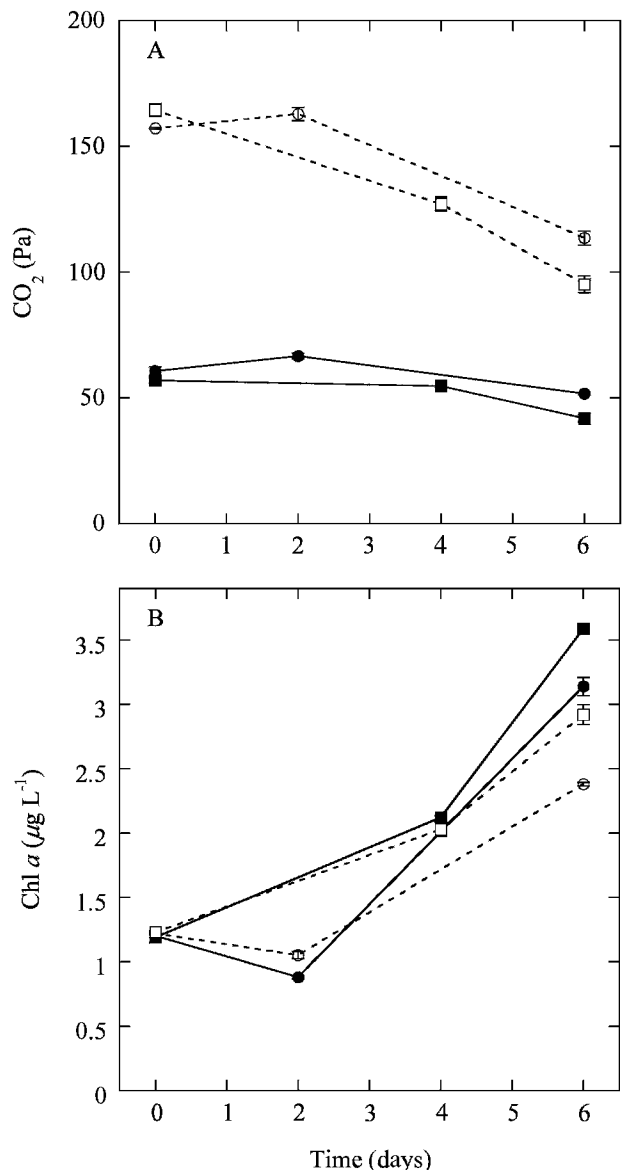
Fig. 1. Changes in (A) CO_2 partial pressure (Pa), and (B) chlorophyll accumulation, Chl *a* (μg L^{-1}) in Lake Giles microcosms incubated at 3 m in 2005 with and without added CO_2 (mean ± SEM). Open symbols and dashed lines correspond to samples preaerated with 0.1% CO_2 (101.3 Pa, high CO_2) and closed symbols and solid lines correspond to samples without added CO_2 (low CO_2). The circles represent the experiment starting 20 July and the squares those from the experiment starting 21 July. Error bars that are not shown (i.e., closed symbols) correspond to values smaller than the symbols.

Fig. 2. Photosynthesis–irradiance (*P-E*) curves for PAR-only exposure (photosynthetron) obtained for Lake Giles microcosms from 2005 experiments. Open symbols and dashed lines correspond to samples aerated with 0.1% CO_2 (101.3 Pa, high CO_2) and closed symbols and solid lines correspond to samples without added CO_2 (low CO_2). Crossed symbols represent Lake Giles water samples at the start of the incubation. The circles and thin lines correspond to the values from the experiment starting 20 July and the squares and thick lines to those from the experiment starting 21 July. Nonlinear regression was obtained by fitting values to Eq. 1.

10). High CO_2 concentrations produced an increase in P_s^B of 23% compared with low CO_2 concentrations (Table 1). The CO_2 level also affected the light saturation parameter E_s, and the initial slope of the photosynthesis irradiance curves, α ($= P_s^B / E_s$). The latter parameter increased from 0.014 to 0.019 under high CO_2 concentrations, indicating a 36% increase in photosynthetic efficiency (i.e., assimilated carbon : PAR) under these conditions (Table 1).
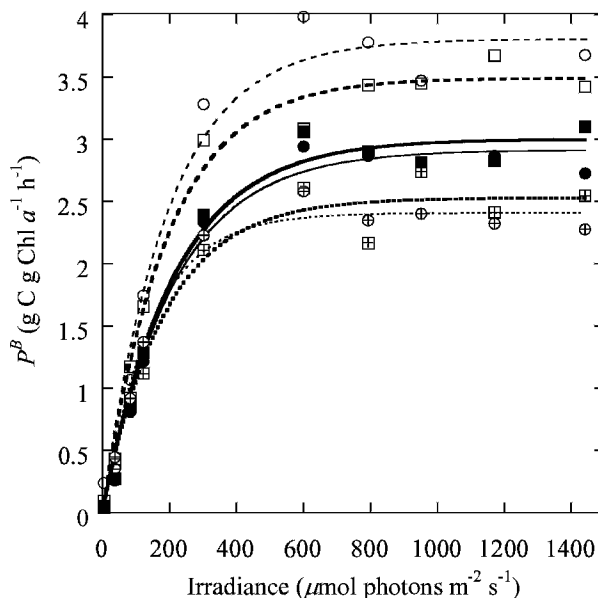
P-E curves obtained from PAR plus UVR exposures in the photoinhibitron showed that carbon fixation in the lake assemblages decreased both at higher irradiance and with the inclusion of shorter wavelengths in the spectra (Figs. 3, 4). Figure 3 shows only the photosynthetic rates obtained using the long-pass filters LG 370 and WG 320 for simplicity as an example of the responses observed in the photoinhibitron. Although photosynthetic rates were always higher under high CO_2, the relative decrease of the photosynthetic rates under photoinhibitory irradiances was more pronounced under high-CO_2 than under low-CO_2 conditions. In addition, photoinhibition was more severe when the spectra included shorter wavelengths, i.e., by using the WG 320 long-pass filter compared with the LG 370. The analysis of the carbon fixation rates for all the spectral treatments ($n = 80$) using the BWF$_T$/*P-E* model (Eq. 2) allowed the estimation of the sensitivity coefficients (or "weights") for each wavelength in both high- and low-CO_2 conditions. The set of weighting coefficients, $\varepsilon(\lambda)$, formed the BWFs for the inhibition of photosynthesis (Fig. 4A). Similar to the trends observed previously with the *P-E* curves using the LG 370 and WG 320 long-pass filters, the BWFs showed that sensitivity of photosynthesis to UVR increased for shorter wavelengths in both high- and low-CO_2 microcosms (Fig. 4A). However, sensitivity to UVR was higher under high-CO_2 concentrations, as shown by the higher values of $\varepsilon(\lambda)$ in the high-CO_2 microcosms. Significant differences in sensitivity to UVR

Table 1. Photosynthetic parameters of Lake Giles water samples incubated for 6 d in July 2005 at 3-m depth with a 0.1% CO_2 enrichment (101.3 Pa, high CO_2) and without the CO_2 enrichment (low CO_2). Lake Giles T_0 (LG(T_0)) corresponds to values obtained from Lake Giles water samples at the start of the in situ incubation. The parameters were estimated using nonlinear regression fitting of Eq. 1 to the values obtained from ^{14}C incubations in the photosynthetron (i.e., only PAR). Values (mean $\pm$ SEM) are the light-saturated rate of photosynthesis, P_s^B (g C [g Chl a]$^{-1}$ h^{-1}), the saturation irradiance, E_s (μmol photons m^{-2} s^{-1}), and the initial slope of the photosynthesis–irradiance curves, α (g C [g Chl a]$^{-1}$ h^{-1} [μmol photons m^{-2} s^{-1}]$^{-1}$). R^2 is the coefficient of determination.

	LG(T_0)	Low CO_2	High CO_2
P_s^B	2.47±0.05	2.96±0.06	3.65±0.09
E_s	166.0±14.6	213.0±16.26	192.5±17.07
α	0.015±0.001	0.014±0.001	0.019±0.002
R^2	0.99	0.99	0.99

were observed between 335 and 370 nm, corresponding to the UVA region of the spectra. Further analysis weighting solar spectral irradiance at the surface by the obtained BWFs showed that for clear-sky exposures at midday, differences in weighted irradiance became significant at longer wavelengths ($\lambda > 315$ nm) due to the greater weights for high-CO_2 treatments at those wavelengths (Fig. 4B). The weighted irradiance spectra ($E^*(\lambda)$) also showed a peak at 330 nm, demonstrating the strong biological effect of this wavelength region. Analyzing ε(330) values as a sensitivity index of photosynthesis to UVR in each replicate, it was observed that sensitivity to UVR increased from the start to the end of the incubation, with samples collected on 21 July having the largest differences between

high- and low-CO_2 conditions (Fig. 5). Photosynthetic rates under ambient irradiance at the surface including both PAR and UVR are predicted (Eq. 2) to be strongly inhibited to 17% of potential (uninhibited) photosynthesis under high-CO_2 levels compared with 21% under usual CO_2 levels in the lake, producing similar photosynthetic rates (i.e., P^B) under high- and low-CO_2 conditions (Table 2).

In experiments performed in summer 2006, *Sphaerocystis* was again the dominant alga, comprising 80% of the total biovolume, whereas *Merismopedia* and *Elakatothrix* represented less than 1%. Numerous other taxa made up the other 19% of biovolume. Algae were incubated near the lake surface, so that there was significant exposure to UVR, and CO_2 enrichment occurred because of the progressive degradation of CDOM by both microbial and photochemical processes. CDOM addition changed the DIC composition and reduced UVR penetration within the sample. Initially, UVA irradiance that reached the interior of the UVR-exposed Teflon bottles was 49% of the incident subsurface irradiance, and UVB was 37%. After 6 d of UV exposure, light attenuation decreased because of photobleaching of CDOM, and UVA and UVB in the Teflon bottle reached values of 68% and 53% of the incident irradiance, respectively. By comparison, UVR exposure of the Lake Giles phytoplankton assemblage (average over 4.3-m surface mixed layer) was 28% and 10% of incident UVA and UVB. DIC also changed after 6 d of incubation from 25.6 μmol L^{-1} in the lake to averages (including both $-$UVR and $+$UVR) of 51.9 μmol L^{-1} and 32.3 μmol L^{-1} in bottles with and without CDOM addition, respectively (Fig. 6A). No significant differences in DIC were observed among samples without CDOM, independent of the spectral treatment or the inclusion of algae as opposed to
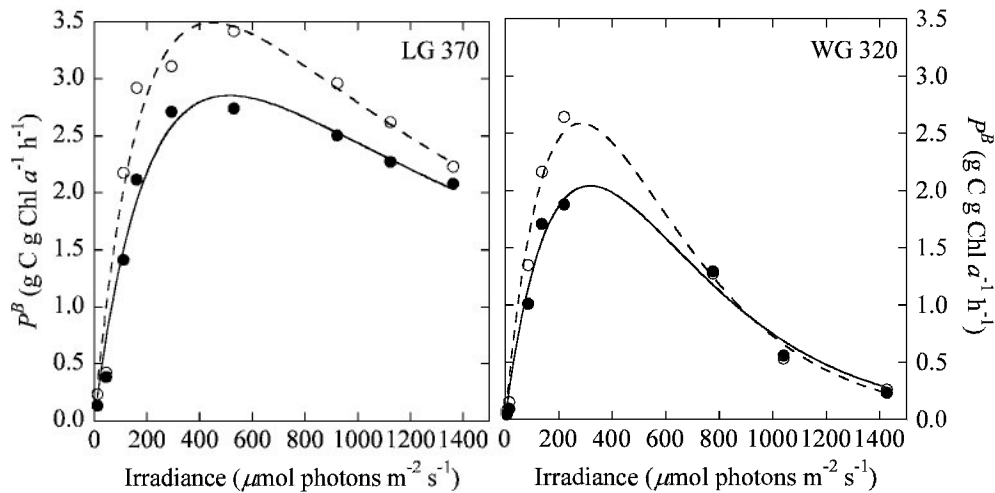

Fig. 3. Photosynthesis–irradiance (*P-E*) curves for PAR+UVR exposures obtained from exposures in the polychromatic incubator (photoinhibitron) using Lake Giles water samples incubated for 6 d at 3 m with and without CO_2 enrichment. Open symbols and dashed lines correspond to phytoplankton aerated with 0.1% CO_2 (101.3 Pa, high CO_2) and closed symbols and solid lines correspond to phytoplankton without added CO_2 (low CO_2). Irradiance is shown only as PAR for simplicity, but LG 370 long-pass filter allowed the transmission of $\lambda > 370$ nm and WG 320 $\lambda > 320$ nm. Associated curves show the trends in each data set (these are not BWF predictions).
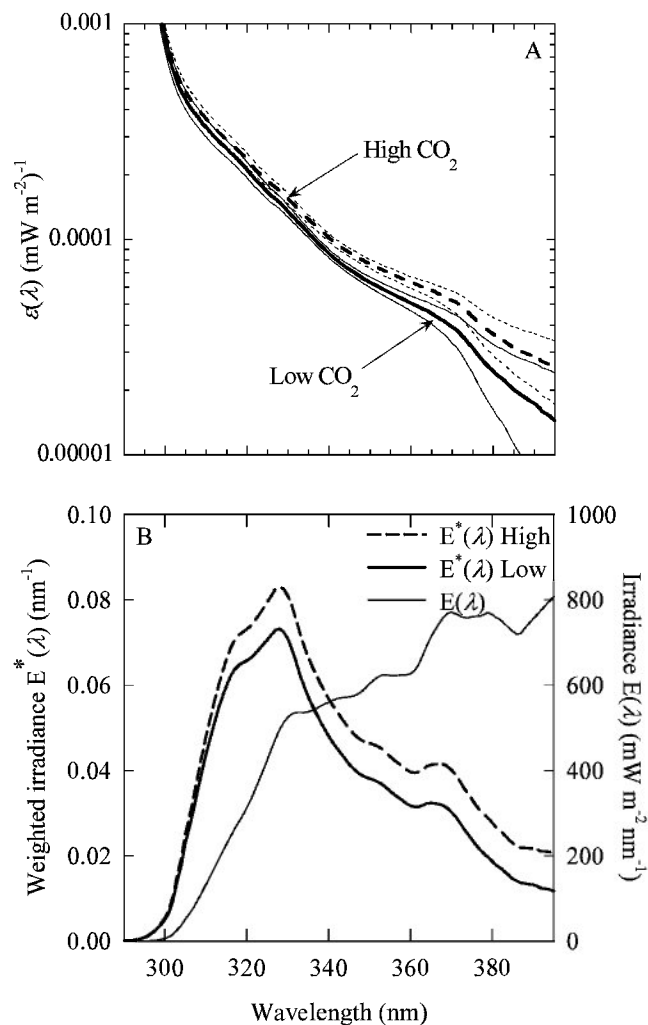
Sobrino et al.

Fig. 4. (A) Average biological weighting functions (BWFs, $\varepsilon(\lambda)$, [mW m^{-2}]$^{-1}$) for the inhibition of photosynthesis in Lake Giles water samples incubated for 6 d at 3 m with and without CO_2 enrichment. Thin lines represent the SEM calculated from error estimates of individual BWFs. (B) UVR spectrum for solar exposures ($E(\lambda)$, mW m^{-2} nm^{-1}) from measurements at Lake Giles during summer at midday combined with radiative transfer model calculations (thin line; see Methods), and weighted spectral irradiances ($E^*(\lambda)$, nm^{-1}) calculated for the same solar spectrum from the average BWFs estimated for Lake Giles phytoplankton incubated with and without CO_2 enrichment (thick lines). The irradiance spectrum was smoothed to aid comparison of $E^*(\lambda)$ spectra.

only bacteria. However, significant differences related to light treatment were observed in the samples with CDOM; when UVR was imposed, DIC reached maximum values of 62.2 μmol L^{-1}. In samples with CDOM, pH declined slightly from 6.02 to average 5.94 as CO_2 partial pressure increased from 47.2 Pa to an average of 101.9 Pa (Fig. 6B). Maximum CO_2 concentrations reached by the UVR-exposed samples were 116.2 Pa in the sample including both phyto- and bacterioplankton, and 126.3 Pa in the sample containing only bacteria (Fig. 6B).

The photosynthetic response in the absence of UVR differed from that observed in the 2005 experiments.
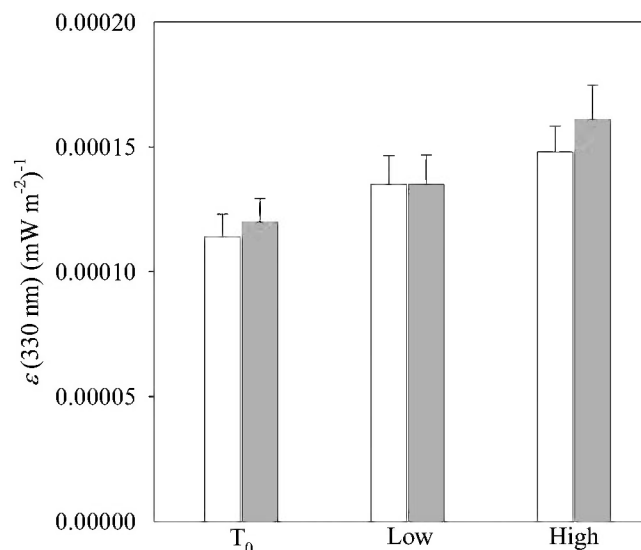

Fig. 5. Sensitivity to UVR measured as the weighting coefficient $\varepsilon(330)$ (mW m^{-2})$^{-1}$ obtained from Lake Giles water samples from 2005 experiments. T_0 corresponds to values obtained from the Lake Giles water sample at the start of the in situ incubation. High CO_2 corresponds to phytoplankton aerated with 0.1% CO_2 (101.3 Pa) and incubated for 6 d at 3 m and low CO_2 to phytoplankton incubated without added CO_2. Open bars are the values from the experiment starting 20 July and the closed bars those from the experiment starting 21 July.

Elevated CO_2 concentrations produced by the CDOM addition after 6 d of incubation did not increase the photosynthetic rates (Table 3); however, differences were observed between treatments exposed to full solar spectrum and those where UVR was excluded. Chl a, P_s^B, and E_s increased 38%, 47%, and 27%, respectively, in phytoplankton assemblages exposed to UVR compared with those without UVR (Table 3).

In contrast, when photosynthesis was assessed in the presence of PAR plus UVR in the photoinhibitron, results were similar to those obtained the previous summer. Phytoplankton from higher CO_2 concentrations showed higher sensitivity to UVR than the phytoplankton from the lake (Fig. 7A). High-CO_2 assemblages acclimated to UVR during the in situ incubation showed lower sensitivity to UVR photoinhibition than high-CO_2 phytoplankton that had been protected from UVR. For phytoplankton incubated with CDOM, comparison of the detailed BWFs instead of a specific value at 330 nm showed that spectral differences between phytoplankton exposed to UVR and those protected from UVR during the incubation were found in the UVA region of the spectrum, consistent with the greater relative transmission of UVA by CDOM (Fig. 7B). Therefore, differences in the spectral sensitivity of photosynthesis arose from higher UVA irradiance inducing acclimation to UVA in the assemblages incubated with CDOM and exposed to the whole solar spectrum compared with those protected from UVR. Similar results were obtained when we estimated the weighted irradiances for a clear day at midday (Table 2). For these conditions, the results also showed that CDOM additions did not

Table 2. Photosynthetic parameters of Lake Giles water samples under UVR. Average weighted irradiance for UVR, expressed as a percentage of that at the surface, associated with the lake surface layer and each incubation ($\%E^*_{inh}$(UVR)), and, for a clear summer day at midday in surface (10 cm depth), weighted irradiances, photosynthetic rates, and percentage photoinhibition for full-spectrum irradiance (i.e., PAR and UVR) estimated for Lake Giles phytoplankton. E^*_{inh} stands for the average weighted irradiance (dimensionless), P^B (g C [g Chl a]$^{-1}$ h^{-1}) corresponds to estimated photosynthetic rates at the surface under solar exposure, $P^B : P^B_S$ is the ratio of solar-inhibited to potential photosynthesis obtained from incubations in the photoinhibitron, and %inh is the percentage inhibition of those samples at surface. LG corresponds to freshly collected samples from Lake Giles (average depth of the mixed layer was 5.1 m and 4.3 m for July 2005 and June 2006, respectively). The symbols + or − stand for the presence or absence of CDOM addition (C) and UV radiation (UV) in samples that were incubated under these conditions for 6 d.

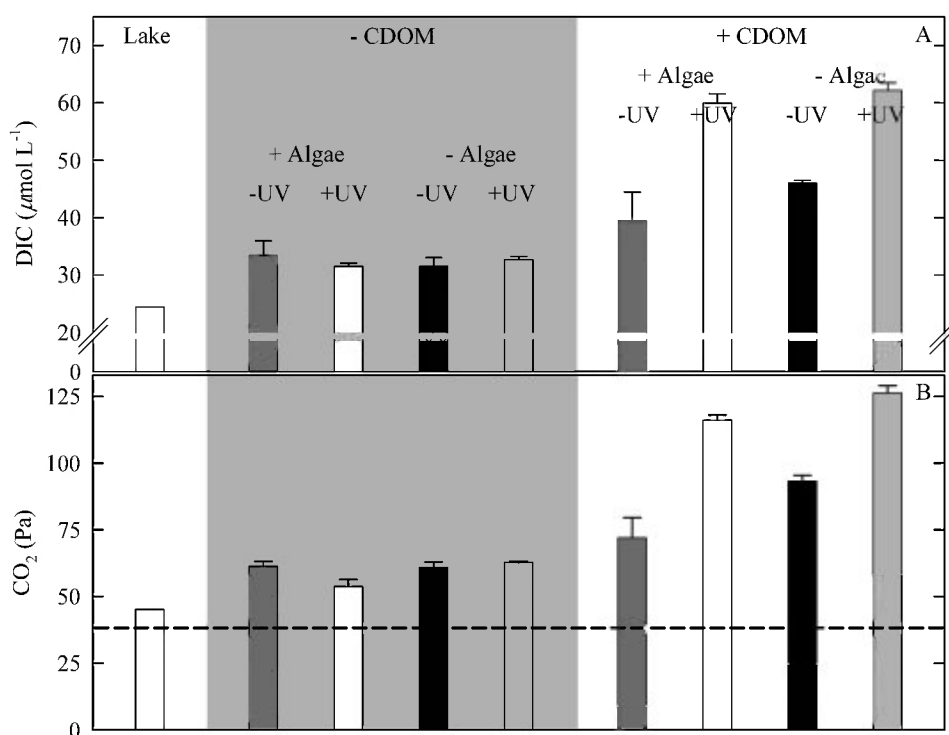|	Treatment	Calculated for midday irradiance at surface			
	$\%E^*_{inh}$(UVR)	E^*_{inh}	P^B	$P^B : P^B_S$	%inh
2005					
LG	23.1	4.29	0.58	0.23	76.7
Low CO$_2$	9.0	4.76	0.62	0.21	79.0
High CO$_2$	10.0	5.88	0.63	0.17	82.8
2006					
LG	17.6	5.52	0.46	0.18	81.6
+C +UV	55.1	9.26	0.26	0.11	89.2
+C −UV	1.7	11.07	0.19	0.09	91.0

Fig. 6. Dissolved inorganic carbon (DIC, μmol L^{-1}) and CO$_2$ partial pressures (CO$_2$, Pa) measured in samples collected from Lake Giles and incubated in Teflon bottles at the surface (10 cm) for 6 d for experiments carried out in 2006 (mean ± SEM). Lake denotes freshly collected Lake Giles water samples. The symbols + or − denote the presence or absence of added CDOM, algae (by filtering through 1-μm filter), and UV radiation (UV). The dashed line in the lower plot indicates saturated dissolved CO$_2$ partial pressure for surface water under the 2005–2006 atmosphere (pCO$_2$ = 38.50 Pa).

Table 3.   Chl *a* content (μg L^{-1}), CO_2 partial pressure pCO$_2$ (Pa), and photosynthetic parameters (*see* Table 1 legend) of Lake Giles water samples from June 2006 experiment. LG corresponds to values obtained from freshly collected samples from Lake Giles. The symbols + or $-$ stand for the presence or absence of CDOM addition (C) and UV radiation (UV) in the Teflon bottles incubated in surface (10 cm average depth) for 6 d.

	Chl *a*	pCO$_2$	P_s^B	E_S	α	R^2
LG	0.63±0.01	47.2±0.8	2.51±0.07	136±13	0.0185	0.97
$-$C +UV	1.17±0.11	53.8±2.5	2.11±0.06	136±13	0.0155	0.96
$-$C $-$UV	0.73±0.04	61.3±1.9	1.60±0.04	109±13	0.0146	0.95
+C +UV	0.89±0.11	116.2±18.5	2.36±0.06	131±12	0.0180	0.97
+C $-$UV	0.76±0.03	72.0±7.6	1.57±0.03	102±9	0.0153	0.97

increase photosynthetic rates independently of the presence of UVR or despite the high CO_2 concentrations (Table 2). Photoinhibition by midday surface irradiance varied from 82% to 91% of maximum photosynthesis obtained in the absence of damage (Table 2), and with PAR responsible for only 5% of total photoinhibition (data not shown).

Discussion

This study demonstrates that a rise in atmospheric CO_2 concentrations similar to that predicted for the end of the century (IPCC 2001) can increase primary productivity in natural lake waters up to 23% in the absence of photoinhibition. However, cells acclimated to high CO_2 concentrations become more sensitive to photoinhibition than those under present atmospheric levels of CO_2, reducing the observed increase in primary productivity when cells are exposed to photoinhibitory UVR. These findings are similar to the results obtained from the estuarine diatom *T. pseudonana* grown in the laboratory under controlled conditions (Sobrino et al. 2008), but this is the first report of this type of response for natural phytoplankton assemblages incubated in situ. Furthermore, the increase in sensitivity to UVR under high-CO_2 conditions occurred in two different scenarios, when CO_2 was enhanced both by aeration with a CO_2–air mixture and under high CO_2 levels produced by the mineralization of terrestrial-derived CDOM. In both cases carbon fixation was assessed after allowing at least 4 d for physiological adjustment to a step increase in CO_2, after which cells reached a steady state comparable with that expected under a progressive increase in CO_2 (Sobrino et al. 2008).

The experiments performed in 2005, where the only experimental factor contributing to changes in the photosynthetic metabolism was the increase in the external CO_2 concentrations, demonstrated that the increase in the maximum photosynthetic rates under high CO_2 levels compared with those under low CO_2 levels was accompanied by a significant increase in photosynthetic efficiency (α). This response has been previously related to a decrease in the activity of the CO_2-concentrating mechanisms of phytoplankton, which reduces the energy required to fix carbon (Berman-Frank et al. 1998). Decreases in cellular Chl *a* content, carbonic anhydrase and ribulose-1,5-bisphosphate carboxylase/oxygenase activity, and the size of the intracellular pools of photosynthetic intermediates also have been described for phytoplankton after acclimation to

elevated CO_2 conditions (Aizawa and Miyachi 1986; Berman-Frank et al. 1998; Sobrino et al. 2008). These cellular changes seem to indicate that high CO_2 levels promote the downregulation of the photosynthetic machinery in phytoplankton, increasing the resource use efficiency, as proposed in previous theoretical studies (Raven 1991). In fact, the lower accumulation of chlorophyll in the lake samples from 2005 incubated with added CO_2 compared with the samples without a CO_2 addition also seems to support this same contention. Nevertheless, changes in taxonomical composition caused by the elevated CO_2 conditions could also contribute to the response observed for the Chl *a*. Among phytoplankton taxa, growth of the cyanobacterium *Merismopedia* was promoted by high CO_2 conditions compared with other phytoplanktonic species. These findings agree with previous studies that show an increased predominance of cyanobacteria in freshwater lakes under predicted scenarios of global change (Jöhnk et al. 2008). It is possible that a downregulated metabolism would have relatively lower amounts of enzymes involved in the repair process of UVR-caused damage or lower activation state of the general defense mechanism (e.g., lower concentrations per cell of superoxide dismutase and ascorbate peroxidase) (Lesser 1996). Reduced amount or activity of the enzymes involved in cellular repair would increase susceptibility to UVR, resulting in more photoinhibition when UVR stress is imposed than would occur in cells with normal metabolic activity (Litchman et al. 2002). Additionally, high-CO_2 conditions could enhance the contribution of UVR-sensitive cellular components to photosynthesis, resulting in more susceptible phytoplankton than under low-CO_2 conditions (Beardall et al. 2002).

Even though the exact mechanisms resulting in the increase in sensitivity under high-CO_2 atmospheric levels have not been elucidated thus far, our results showed that the increase in sensitivity to UVR also can be produced at present atmospheric CO_2 levels by the interaction of natural environmental factors with DOM. Comparable with other, similar lakes, Lake Giles water was supersaturated in CO_2 (47.2 Pa) as a result of the high heterotrophic activity and DOM photomineralization by solar radiation (Cole et al. 1994; Granéli et al. 1996). Remarkably, concentrations of CO_2 increased (to average 59.7 Pa; Fig. 6B) in containers incubated without added CDOM probably because of higher light exposure at the surface and bacterial decomposition of native CDOM. Exclusion
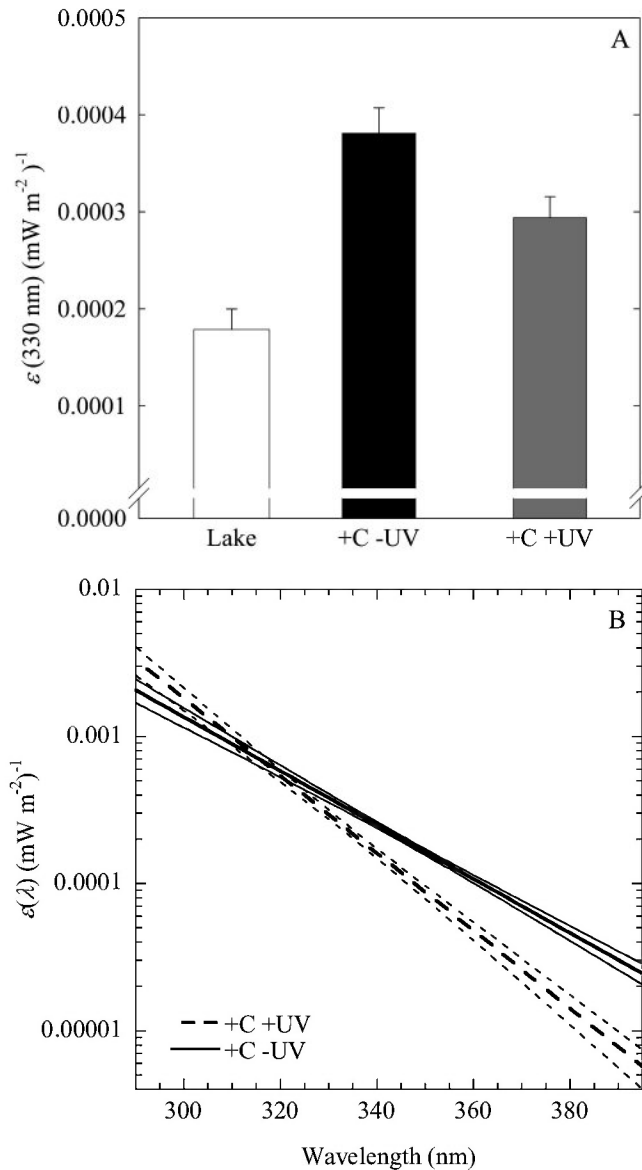
Fig. 7. Sensitivity to UVR measured as (A) the weighting coefficient $\varepsilon(330)$ (mW m^{-2})$^{-1}$ and (B) the biological weighting functions (BWFs, $\varepsilon(\lambda)$, [mW m^{-2}]$^{-1}$) for the inhibition of photosynthesis estimated for phytoplankton assemblages from Lake Giles incubated at the surface in UVR-transparent Teflon bottles (2006 experiments). "Lake" stands for freshly collected Lake Giles water samples. The symbols + or − stand for the presence or absence of added CDOM and UVR. Thin lines represent the SEM calculated from error estimates of individual BWFs.

of UVR did not strongly affect CO_2 production from native CDOM; therefore heterotrophic activity probably accounted for most of the buildup. However, much higher CO_2 production was observed when UVR was included in the spectral exposure of the CDOM-enriched bottles, reaching CO_2 average partial pressures of 116.2 Pa, approximately three times present atmospheric CO_2 levels (38.5 Pa). Our results for the production of CO_2 from mineralization of CDOM are in the range predicted by previous studies (Sobek et al. 2003) but do not quantify to

what extent biomineralization or photodegradation contributed to CO_2 accumulation in our experiments. Photomineralization already has been identified as an important contributor to CO_2 production from the degradation of terrigenous CDOM (Granéli et al. 1996; Moran et al. 2000). Reports show that it can account for the removal of 10–50% of total DOC compared with 10–27% removed by biomineralization (Moran et al. 2000; Lennon 2004; Obernosterer and Benner 2004).

Interestingly, the higher CO_2 concentrations produced by the CDOM addition were not enough to enhance carbon fixation in phytoplankton assemblages where UVR was excluded from the in situ incubation. On the contrary, phytoplankton incubated in the presence of UVR had maximum photosynthetic rates (measured in the absence of UVR) that were 47% higher than the photosynthetic rates of in situ phytoplankton incubated in the absence of UVR (Table 3). Previous studies have demonstrated that UVR can drive the phototransformation of CDOM to bioreactive compounds, increasing the availability of limiting substrates for primary production (Moran and Zepp 1997; Vinebrooke and Leavitt 1998). In Lake Giles, nitrogen and phosphorus tend to colimit epilimnetic phytoplankton Chl a levels in summer, a general finding from multiday nutrient enrichment bioassays, under noninhibitory PAR, including June 2005 and July 2006 (R.E. Moeller unpubl.). So we would expect this community to respond positively to UVR-driven nutrient regeneration.

When in situ photosynthesis was estimated for a clear sky at midday, UVR was calculated to reduce photosynthesis by an average of 78% relative to uninhibited photosynthesis. The contribution of PAR to photoinhibition was much smaller, with average values for both years close to 6% (Table 2). The robustness of the $BWF_T/P\text{-}E$ model used in this study to predict UV- and PAR-dependent photosynthetic responses is supported by average R^2 values close to 0.97, obtained when comparing the observed and the predicted photosynthetic rates. Similar values of UVR–photoinhibition have been also reported for other lakes and estuaries (Helbling et al. 2001; Neale et al. 2001).

Analyzing the causes of the changes in sensitivity to UVR in Lake Giles phytoplankton assemblages in situ was complicated because of the interaction among the different environmental variables. The phytoplankton assemblage from 2005 was less sensitive to UVR than that for 2006, possibly due to lower nutrient concentrations in 2006 inducing lower repair capacity and increasing sensitivity of phytoplankton to UVR (Litchman et al. 2002), and different taxonomic composition. Regarding this, cell counts of the cyanobacteria *Merismopedia* showed an increase under high CO_2 conditions in 2005 incubations. *Merismopedia* was also relatively more abundant in 2005 than in 2006 on the basis of both cell counts and biovolume. Previous studies have shown that UVR exposure promotes phytoplankton photoacclimation to UVR, decreasing sensitivity to UVR (Fritz et al. 2008; Sobrino et al. 2008), whereas an artificial addition of CO_2 increases sensitivity (Sobrino et al. 2008). Additionally, CDOM addition can increase the sensitivity to UVR both through reduction of UVR photoacclimation and irradi-

ance in general (Villafañe et al. 2004), as well as the production of CO_2 from photobleaching (this study). Because of this, we observed the highest sensitivity to UV in the treatment with added CDOM and no UVR exposure. This was despite an even higher CO_2 concentration in the UVR exposed treatment.

In conclusion, the results from this study show that high CO_2 concentrations can increase primary productivity in lake phytoplankton assemblages even in the presence of a presumed nutrient limitation. However, elevated CO_2 conditions, caused by changes in atmospheric concentrations or by UVR photodegradation of CDOM, increase sensitivity to UVR, making cells more susceptible to photoinhibition than those under present or nonelevated CO_2 levels. The overall effect on a water column basis will depend on the relative proportion between a near-surface photoactive zone where UVR can drive increased availability of nutrients and CO_2 but lower productivity, and a deeper zone where UVR is absent but PAR can drive higher rates of photosynthesis in response to the nutrient and CO_2 enhancements. In addition, the confirmation of these results in other systems can imply the presence of more sensitive phytoplankton, independently of the source of damage, in future scenarios of global climate change and in waters presently enriched with high CO_2 concentrations. Future efforts should be made to understand the physiological mechanisms of this increase in sensitivity, estimate its effect on integral water column production, and assess interactions with other environmental stressors under elevated CO_2 conditions. Finally, the effect of elevated atmospheric CO_2 concentrations on waters with significant inputs of organic matter still needs to be studied.

References

AIZAWA, K., AND S. MIYACHI. 1986. Carbonic anhydrase and CO_2 concentrating mechanisms in microalgae and cyanobacteria. FEMS Microbiol. Rev. **39:** 215–233.

BEARDALL, J., P. HERAUD, S. ROBERTS, K. SHELLY, AND S. STOJKOVIC. 2002. Effects of UVB radiation on inorganic carbon acquisition by the marine microalga *Dunaliella tertiolecta* (Chlorophyceae). Phycologia **41:** 268–272.

BERMAN-FRANK, I., J. EREZ, AND A. KAPLAN. 1998. Changes in inorganic carbon uptake during the progression of a dinoflagellate bloom in a lake ecosystem. Can. J. Bot. **76:** 1043–1051.

COLE, J. J., N. F. CARACO, G. W. KLING, AND T. K. KRATZ. 1994. Carbon dioxide supersaturation in the surface waters of lakes. Science **265:** 1568–1570.

CULLEN, J. J., AND P. J. NEALE. 1997. Biological weighting functions for describing the effects of UV radiation on aquatic systems, p. 97–118. *In* D. P. Häder [ed.], The effects of ozone depletion on aquatic ecosystems. Landes.

———, ———, AND M. P. LESSER. 1992. Biological weighting function for the inhibition of phytoplankton photosynthesis by UV radiation. Science **258:** 646–650.

DE LANGE, H. J., D. P. MORRIS, AND C. E. WILLIAMSON. 2003. Solar ultraviolet photodegradation of DOC may stimulate freshwater food webs. J. Plank. Res. **25:** 111–117.

FRITZ, J. J., P. J. NEALE, R. F. DAVIS, AND J. A. PELOQUIN. 2008. Response of Antarctic phytoplankton to solar UVR exposure: Inhibition and recovery of photosynthesis in coastal and pelagic assemblages. Mar. Ecol. Prog. Ser. **365:** 1–16.

GRANÉLI, W., M. LINDELL, AND L. TRANVIK. 1996. Photooxidative CO_2 production in lakes of different humic content. Limnol. Oceanogr. **41:** 698–706.

HAUER, F. R., AND OTHERS. 1997. Assessment of climate change and freshwater ecosystems of the Rocky Mountains, USA and Canada. Hydrol. Proc. **11:** 903–924.

HEIN, M., AND K. SAND-JENSEN. 1997. CO_2 increases oceanic primary production. Nature **388:** 526–527.

HELBLING, E. W., V. E. VILLAFAÑE, A. G. J. BUMA, M. ANDRADE, AND F. ZARATTI. 2001. DNA damage and photosynthetic inhibition induced by solar ultraviolet radiation in tropical phytoplankton (Lake Titicaca, Bolivia). Eur. J. Phycol. **36:** 157–166.

HINTON, M. J., S. L. SCHIFF, AND M. C. ENGLISH. 1997. The significance of storms for the concentration and export of dissolved organic carbon from two Precambrian Shield catchments. Biogeochemistry **36:** 67–88.

IBELINGS, B. W., AND S. C. MABERLY. 1998. Photoinhibition and the availability of inorganic carbon restrict photosynthesis by surface blooms of cyanobacteria. Limnol. Oceanogr. **43:** 408–419.

IPCC (INTERGOVERNMENTAL PANEL ON CLIMATE CHANGE). 2001. Climate change 2001: The scientific basis. Cambridge. http://www.grida.no/publications/other/ipcc_tar/?src=/climate/ipcc_tar/wg1/518.htm

JANKOWSKI, J. J., D. J. KIEBER, AND K. MOPPER. 1999. Nitrate and nitrite ultraviolet actinometers. Photochem. Photobiol. **70:** 319–328.

JÖHNK, K., J. HUISMAN, J. SHARPLES, B. SOMMEIJER, P. VISSER, AND J. STROOM. 2008. Summer heatwaves promote blooms of harmful cyanobacteria. Global Change Biol. **14:** 495–512.

LENNON, J. T. 2004. Experimental evidence that terrestrial carbon subsidies increase CO_2 flux from lake ecosystems. Oecology **138:** 584–591.

LESSER, M. P. 1996. Elevated temperatures and ultraviolet radiation cause oxidative stress and inhibit photosynthesis in symbiotic dinoflagellates. Limnol. Oceanogr. **41:** 271–283.

LEWIS, M. R., AND J. C. SMITH. 1983. A small volume, short incubation-time method for measurement of photosynthesis as a function of incident irradiance. Mar. Ecol. Prog. Ser. **13:** 99–102.

LITCHMAN, E., P. J. NEALE, AND A. T. BANASZAK. 2002. Increased sensitivity to ultraviolet radiation in nitrogen-limited dinoflagellates: Photoprotection and repair. Limnol. Oceanogr. **47:** 86–94.

MORAN, M. A., W. M. SHELDEON, AND R. G. ZEPP. 2000. Carbon loss and optical property changes during long-term photochemical and biological degradation of estuarine dissolved organic matter. Limnol. Oceanogr. **45:** 1254–1264.

———, AND R. G. ZEPP. 1997. Role of photoreactions in the formation of biologically labile compounds from dissolved organic matter. Limnol. Oceanogr. **42:** 1307–1316.

NEALE, P. J. 2000. Spectral weighting functions for quantifying the effects of UV radiation in marine ecosystems, p. 72–100. *In* S. J. de Mora, S. Demers and M. Vernet [eds.], The effects of UV radiation on marine ecosystems. Cambridge Univ. Press.

———, AND J. J. FRITZ. 2001. Experimental exposure of plankton suspensions to polychromatic UV radiation for determination of spectral weighting functions, p. 291–296. *In* J. Slusser, J. R. Herman and W. Gao [eds.], UV ground- and space-based measurements, models, and effects. SPIE—The International Society for Optical Engineering.

———, AND OTHERS. 2001. Quantifying the response of phytoplankton photosynthesis to ultraviolet radiation: Biological weighting functions versus in situ measurements in two Swiss lakes. Aquat. Sci. **63:** 265–285.

OBERNOSTERER, I., AND R. BENNER. 2004. Competition between biological and photochemical processes in the mineralization of dissolved organic carbon. Limnol. Oceanogr. **49:** 117–124.

PECHAR, L. 1987. Use of an acetone:methanol mixture for the extraction and spectrophotometric determination of chlorophyll-a in phytoplankton. Arch. Hydrobiol. Beih. Ergebn. Limnol. **28:** 99–117.

PIENITZ, R., AND W. F. VINCENT. 2000. Effect of climate change relative to ozone depletion on UV exposure in subarctic lakes. Nature **404:** 484–487.

RAVEN, J. A. 1991. Physiology of inorganic C acquisition and implications for resource use efficiency by marine phytoplankton: Relation to increased CO_2 and temperature. Plant Cell Environ. **14:** 779–794.

RIEBESELL, U., I. ZONDERVAN, B. ROST, P. D. TORTELL, R. ZEEBE, AND F. M. M. MOREL. 2000. Reduced calcification of marine plankton in response of increased atmospheric CO_2. Nature **407:** 364–367.

RUGGABER, A., R. DLUGI, AND T. NAKAJIMA. 1994. Modeling radiation quantities and photolysis frequencies in the troposphere. J. Atmos. Chem. **18:** 171–210.

RUNDEL, R. D. 1983. Action spectra and estimation of biologically effective UV radiation. Physiol. Plant. **58:** 360–366.

SABINE, C. L., AND OTHERS. 2004. The oceanic sink for anthropogenic CO_2. Science **305:** 367–371.

SETLOW, R. B. 1974. The wavelengths in sunlight effective in producing skin cancer: A theoretical analysis. Proc. Natl. Acad. Sci. USA **81:** 3363–3366.

SOBEK, S., G. ALGESTEN, A. BERGSTRÖM, M. JANSSON, AND L. J. TRANVIK. 2003. The catchment and climate regulation of pCO_2 in boreal lakes. Global Change Biol. **9:** 630–641.

SOBRINO, C., AND P. J. NEALE. 2007. Short-term and long-term effects of temperature on phytoplankton photosynthesis under UVR exposures. J. Phycol. **43:** 426–436.

———, ———, AND L. M. LUBIÁN. 2005. Interaction of UV radiation and inorganic carbon supply in the inhibition of photosynthesis: Spectral and temporal responses of two marine picoplankters. Photochem. Photobiol. **81:** 384–393.

———, M. L. WARD, AND P. J. NEALE. 2008. Acclimation to elevated CO_2 and ultraviolet radiation in the diatom *Thalassiosira pseudonana*: Effects on growth, photosynthesis and spectral sensitivity of photoinhibition. Limnol. Oceanogr. **56:** 494–505.

STAINTON, M. P. 1973. A syringe gas-stripping procedure for gas chromatographic determination of dissolved inorganic and organic carbon in fresh water and carbonate in sediments. J. Fish. Res. Board Can. **30:** 1441–1445.

SUN, L., E. M. PURDUE, AND J. F. MCCARTHY. 1995. Using reverse osmosis to obtain organic matter from surface and ground waters. Water Res. **29:** 1471–1477.

TORTELL, P. D., AND F. M. M. MOREL. 2002. Sources of inorganic carbon for phytoplankton in the eastern Subtropical and Equatorial Pacific Ocean. Limnol. Oceanogr. **47:** 1012–1022.

VILLAFAÑE, V. E., A. G. J. BUMA, P. BOELEN, AND E. W. HELBLING. 2004. Solar UVR-induced DNA damage and inhibition of photosynthesis in phytoplankton from Andean lakes of Argentina. Archiv. Hydrobiol. **161:** 245–266.

VINEBROOKE, R. D., AND P. R. LEAVITT. 1998. Direct and interactive effects of allochthonous dissolved organic matter, inorganic nutrients, and ultraviolet radiation on an alpine littoral food web. Limnol. Oceanogr. **43:** 1065–1081.

ZEEBE, R. E., AND D. WOLF-GLADROW. 2001. CO_2 in seawater: Equilibrium, kinetics, isotopes. Elsevier Oceanography Series.

ZEPP, R. G., T. V. CALLAGHAN, AND D. J. ERICKSON. 1995. Effects of increased solar ultraviolet radiation on biogeochemical cycles. Ambio **24:** 181–187.

———, D. J. ERICKSON III, N. D. PAUL, AND B. SULZBERGER. 2007. Interactive effects of solar UV radiation and climate change on biogeochemical cycling. Photochem. Photobiol. Sci. **6:** 286–300.

Associate editors: Warwick F. Vincent and John P. Smol